

Research Article

Open Access

Valery I. Arkhipenko, Andrey A. Kirillov, Leanid V. Simonchik*,
Yauhen A. Safronau, Andrey P. Chernukho, Aleksey N. Migoun

Atmospheric pressure glow discharge in air used for ethanol conversion: experiment and modelling

Abstract: Complex theoretical and experimental investigation of ethanol into syngas conversion assisted by DC atmospheric pressure discharge with plasma cathode is presented. Infrared absorption spectroscopy together with the equation for the conservation of the number of atoms at the inlet and outlet of the reactor are used to determine the composition of syngas, the main components of which are hydrogen, carbon monoxide, methane and acetylene. It is shown that the plasma-chemical reactor enables efficient (over 90%) ethanol into syngas conversion with an output of 2 L min⁻¹ and at energy costs of about 3 electron-volts per one hydrogen molecule. Numerical modeling of conversion kinetics at discharge conditions was performed assuming thermal nature of the process. Experimental and calculated data are in good agreement.

Keywords: plasma reforming, syngas, chemical modeling

DOI: 10.1515/chem-2015-0037

received January 30, 2014; accepted May 30, 2014.

1 Introduction

Limited natural resources, especially oil, constantly stimulate research and development of technologies for their most effective use. Theoretical and experimental studies of the influence of hydrogen and synthesis gas addition to the main fuel revealed a high efficiency of this method to improve the performance of classic internal

combustion engine [1,2] at relatively small changes in the motor itself. Hydrogen molecules have a relatively high mobility, which results in their high rate of diffusion and heat conduction. Besides, they play a key role in the chemistry of hydrocarbon combustion. Therefore, one can observe the mentioned performance increase at relatively “simple” adding of hydrogen into the intake manifold.

Due to the problems of storage and transportation of hydrogen a partial oxidation of engine fuels is a promising way to generate hydrogen directly before utilization. Among the possible implementations of hydrogen generators based on this process, a special place is occupied by plasma systems where the process could be fully or partially maintained by plasma [3–5]. The main advantages of technologies based on the use of plasma include the acceptable regimes of operation (atmospheric pressure, low gas temperature), quick start, compact size, etc. Different types of atmospheric pressure discharges (corona, spark, a barrier, gliding arc at DC, AC and pulsating current of different frequency bands) are proposed as plasma sources for these purposes [6–11].

This paper is focused on ethanol to syngas conversion assisted by a DC atmospheric pressure discharge with plasma cathode [12,13]. Along with the description of the facility, experimental conditions and measurements we present the results of mathematical modeling of the process under consideration which are obtained using the same approach as explained in [14], although the kinetic mechanism for ethanol conversion applied as listed in [15].

2 Experimental procedure

The design of plasma-chemical reactor is based on a three-electrode system, which was developed in [12,13] for generation of stable volumetric gas discharges in various atomic and molecular gases. The reactor consists of three-sectional (A, B and C) discharge chamber 1 (Fig. 1a). In section A both cooled tungsten cathode 2 (6 mm diameter rod with a working part rounded at radius of 3 mm) and

*Corresponding author: Leanid V. Simonchik: B.I. Stepanov Institute of Physics of NAS of Belarus 220072 Minsk, Belarus, E-mail: l.simonchik@dragon.bas-net.by

Valery I. Arkhipenko, Andrey A. Kirillov, Yauhen A. Safronau: B.I. Stepanov Institute of Physics of NAS of Belarus 220072 Minsk, Belarus

Andrey P. Chernukho, Aleksey N. Migoun: Private R&D Enterprise «Advanced Research & Technologies», 223058 Leskovka, Belarus

copper anode 3 (plate thickness of about 1 mm) are located at a distance of 1 mm. Power supply U1 (output voltage of 1500 V, the ballast resistance $R1 \sim 1200 \Omega$) is used to ignite a self-sustained glow discharge at a current of 200 mA between these electrodes. The airflow is provided through section A at a rate of up to 0.4 liter per minute. Air output takes place through the hole (diameter 2 mm) in the center of electrode 3 into section C (quartz tube 5 with the diameter of 10 mm and 15 mm long) located under this hole.

Self-sustained DC normal glow discharge [16] in section A served as a plasma cathode for the non-self-sustained discharge in section C which was ignited between electrode 3 and additional electrode 4 located at a distance of 15 mm. This discharge is powered by the second power supply U2 (3000 V, $R2 \sim 1000 \Omega$) in such a manner that additional electrode is an anode.

A mixture of ethanol and water is fed into the chamber together with airflow at a rate of 0.4 liter per minute using the same input canal. Ethanol and water evaporate due to the heating of electrode 4 by the discharge, after that the air-vapor mixture spreads along section B and mixes with airflow from section A and goes into section C. At a discharge current of about 130 mA the positive column plasma fills almost the whole volume of section C (Fig. 1b).

The yield of gases from section C takes place through the hole (diameter of 2 mm) in anode 4 (Fig. 1a) into a copper tube (internal diameter 3 mm). In Fig. 1c the photograph of the plume of exhaust gases combustion at the end of the tube is presented. The length of the flame can reach up to 10 cm, while its color is blue.

The composition of conversion products of the mixture after processing in the plasma reactor was determined by diagnostics based on infrared (IR) absorption spectroscopy [17]. For this purpose, we used infrared spectrometer NEXUS (Thermo Nicolet). The absorption spectra were recorded in the range of $600 - 4000 \text{ cm}^{-1}$ with the resolution of 2 cm^{-1} . Triangular apodization function was chosen, which leads to the diffraction contours of the lines [18]. For spectroscopic analysis, the exhaust gases from the plasma-chemical reactor have passed through 5.7 - centimeter cuvette, which was previously heated up to 90°C in order to prevent condensation of water and alcohol vapors. The hydrogen concentration in the conversion products was additionally controlled by the device described in [17] based on the passage of hydrogen through a palladium membrane [19].

3 Results and discussion

For conversion in the experiment we used the mixture of ethanol (85%) with water (15%), which was fed into the reactor at a rate of 1.25 mL min^{-1} . The total airflow rate was 0.8 L min^{-1} . As a result, the reaction mixture composition at section C input can be estimated as follows: 57% of air, 30% of ethanol vapor and 13% of water vapor. Parameters of the discharges are as follows: sustaining discharge in section A – voltage is 380 V at discharge current of 0.15 A, that corresponds to the electrical power of about 55 W; the main discharge in section C – discharge current equals 0.13 A, the voltage is 1500 V, and, accordingly the power is about 195 W.

Intense vibrational-rotational bands of ethanol ($900, 1050, 1250, 1400, 2950$ and 3700 cm^{-1}), water vapor (1600 cm^{-1} , 3750 cm^{-1}), and much weaker bands of carbon dioxide molecules as a component of the used ambient air are only observed in IR absorption spectrum (Fig. 2a) for the initial reaction mixture. After processing in plasma intense bands of CO (2200 cm^{-1}), CH_4 (3100 cm^{-1}), C_2H_2 (750 and 3300 cm^{-1}), C_2H_4 (950 cm^{-1}) and CO_2 (740 and 2400 cm^{-1}) are observed (Fig. 2 b) in the spectrum of the mixture leaving the reactor. The weak intense absorption bands of ethanol and water are present in the spectrum, as well.

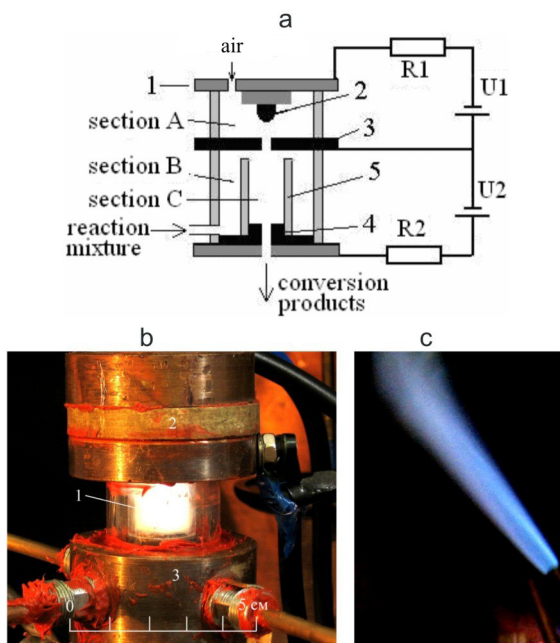


Figure 1: Schematic of plasma-chemical reactor (a) and photos of discharge during ethanol conversion (b) and flame at the reactor output (c).

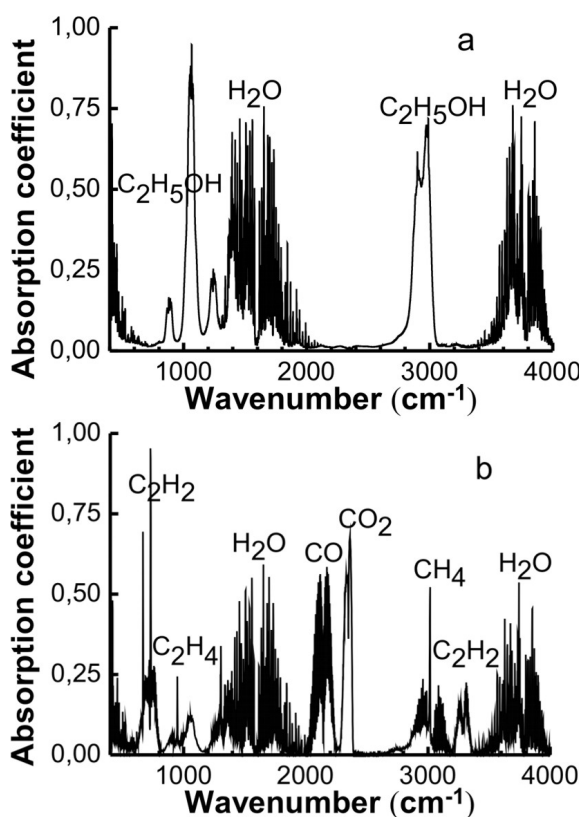


Figure 2: Absorption IR-spectra of mixtures at inlet (a) and outlet (b) of plasma reactor.

Excluding ethanol, mole fractions of all IR active components in the exhaust mixture were determined by the comparison of the experimentally obtained spectrum with the calculated one. The calculated absorption spectrum was plotted using the Hitran database [20]. The mole fraction of ethanol was determined by experimental calibration curve of absorption, plotted using the gas mixtures with known concentrations of ethanol. The molar fractions of conversion products determined as follows $\{C_2H_5OH\} = 0.3\%$, $\{H_2O\} = 8\%$, $\{CO\} = 23\%$, $\{CO_2\} = 1.0\%$, $\{CH_4\} = 1.2\%$, $\{C_2H_2\} = 0.8\%$, $\{C_2H_4\} = 0.4\%$.

As it follows from the examination of IR absorption spectra (Fig. 2b) of ethanol conversion products, the additional gas components with a noticeable percentage which could appear in IR spectra are absent. In addition to leaving the reactor above-mentioned IR active components, the exhaust mixture naturally contains homonuclear molecules of hydrogen, nitrogen and oxygen. Mole fractions of these components were calculated taking into account the composition of the reaction mixture at the inlet of the reactor and the mole fractions of IR active components in the exhaust products determined experimentally.

So, we know the molar concentration of carbon components which allows us to determine the number of carbonaceous molecules leaving the plasma reactor during one minute and distribute between them the number of carbon atoms containing in the input reaction mixture. Now, knowing the ratio of molar concentrations of water and carbon-containing component, it is easy to get the number of water molecules. Then, taking into account an equality of the number of hydrogen, oxygen and nitrogen atoms in the inlet and outlet mixtures, one can easily calculate the number of relevant molecules leaving the plasma reactor per unit time, and determine the appropriate molar concentrations, which are as follows: $\{H_2\} = 36\%$, $\{O_2\} = 0.1\%$, $\{N_2\} = 21\%$.

Using the method for determining H₂ concentration in gaseous mixtures [17] based on the rate of hydrogen diffusion through the palladium membrane into an initially evacuated volume, we obtain $\{H_2\} = 35\%$, which is close to the molar fraction of hydrogen calculated from IR spectroscopic data.

Summing up molar concentrations of all gas components leaving the reactor, we obtain 92 % instead of 100%, which indicates that corresponding experimental data used in the estimations may have been obtained with some error.

Productions of ethanol conversion products are $G(H_2) = 1.2 \text{ L min}^{-1}$, $G(CO) = 0.75 \text{ L min}^{-1}$, $G(CH_4) = 0.04 \text{ L min}^{-1}$ and $G(C_2H_2) = 0.025 \text{ L min}^{-1}$. The total production of syngas is 2.0 L min^{-1} . The ethanol to hydrogen conversion efficiency can be described by

$$\eta(H_2) = \frac{\text{number of H-atoms in generated hydrogen molecules } H_2}{\text{number of H-atoms in ethanol molecules}}, \quad (1)$$

According to Eq. 1 we obtain $\eta(H_2) = 88\%$. Similarly, one can determine the coefficients of ethanol conversion into hydrogen, methane and acetylene, and calculate the total ethanol conversion coefficient, which is 95%. Energy efficiency is determined by the formula

$$\alpha = \frac{\text{energy release at the burning of } H_2, CO, CH_4, C_2H_2}{\text{total electric energy for plasma maintenance}}. \quad (2)$$

Taking into account the total electric power needed for the maintenance of both the self-sustained and non-self-sustained discharges, which is about 250 W, we obtain $\alpha = 1.85$. The energy cost per molecule of hydrogen is approximately 3 eV.

A large amount of energy $\sim 10 \text{ J cm}^{-3}$ is inputted into the gas mixture under the considered conditions, which leads to a significant heating of the gas mixture. Our estimations give the value as high as 2500 K for translational gas temperature, which could be even

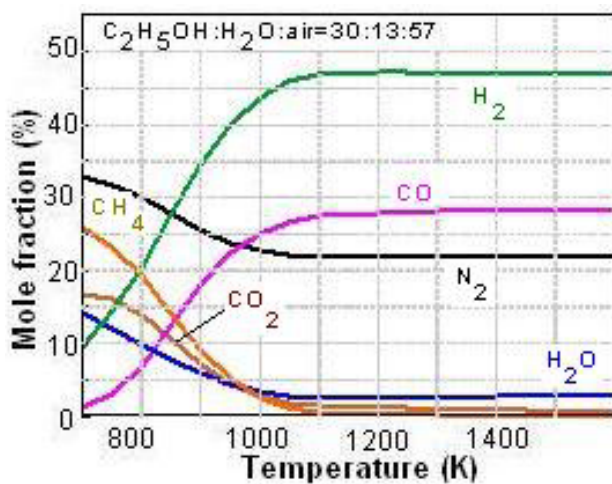


Figure 3: Equilibrium mixture composition against gas temperature.

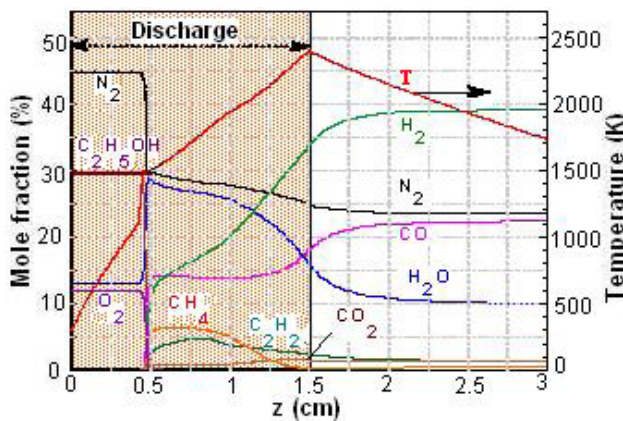


Figure 4: Axial concentration and temperature profiles in reactor.

higher. In this case ethanol conversion most likely has a thermal nature.

Fig. 3 demonstrates the results of thermodynamic calculations of equilibrium concentrations of ethanol conversion products as a function of temperature. It is seen that equilibrium degree of ethanol to hydrogen conversion grows as the gas temperature increases and saturates at $T>1100$ K. This means that from the thermodynamical point of view, the gas temperature of 1100 K is sufficient to have almost maximum conversion degree $\sim 108\%$, where even a part of water vapor is transformed into hydrogen. Nevertheless a question arises whether the intensity of chemical kinetic processes and the residence time are enough to achieve such deep conversion.

To answer this question we performed numerical modeling of conversion kinetics at discharge conditions. It was assumed that 65–70% of discharge energy goes

Table 1: Comparison of experimental and calculated results.

Species	Content, vol. %				
	Initial	Final	Measured, normalized	Calculated, HL=35%	Calculated, HL=30%
$\text{C}_2\text{H}_5\text{OH}$	30	0.3	0.33	0	0
H_2O	13	8	8.81	10.1	6.42
N_2	45.03	21	23.13	23.8	22.7
O_2	11.97	0.1	0.11	0	0
CO	23	23	25.33	22.5	25.5
CO_2	1	1	1.10	1.34	0.89
CH_4	1.2	1.2	1.32	0.67	0.38
C_2H_2	0.8	0.8	0.88	1.5	0.86
C_2H_4	0.4	0.4	0.44	0.12	0.10
H_2	35	35	38.55	39.3	42.9
Total	90.8	100	99.33	99.75	
Conversion	88		82.7	94.7	

into heating of air, water and ethanol, taking into account phase transitions, and the rest is lost by radiation and heat exchange with ambient. Detailed kinetic mechanism of Konnov [15], which consists of 1207 reversible elementary reactions between 127 chemical components, was used in the calculations.

Fig. 4 shows the calculated spatial distribution of the considered system properties. The discharge zone is also denoted in the figure. It is clear that gas mixture heating occurs at the first third of discharge gap.

After that, at about $z=0.5$ cm and $T\sim 1100$ K, one can observe ignition of ethanol followed by a rapid exothermic stage, where water vapor and products of partial ethanol conversion (CH_4 , C_2H_2 , C_2H_4 , etc.) are formed. The rapid exothermic stage is followed by rather slow endothermic one, which we can see at the rest of the discharge gap and in the afterglow, where the products of partial conversion react with water vapor, e.g. $\text{CH}_4 + \text{H}_2\text{O} \rightarrow \text{CO} + 3\text{H}_2$.

For the comparison purposes, Table 1 summarizes experimental and theoretical data on the final composition of the conversion products. Theoretical data were calculated for two values of heat losses (HL) into ambient – 30 and 35%. It is seen that the calculated data are in a good agreement with experimental data for gas mixture composition and hydrogen conversion degree, which is the evidence of adequacy of the theoretical model which was used. It also confirms the initial assumption about

thermal nature of ethanol conversion in the considered conditions.

4 Conclusions

The results of performed experiments show that it is possible to create a compact effective generator based on DC atmospheric pressure discharge with plasma cathode for syngas production operating at comparably low electrical power consumption of 200–250 W and relatively low voltages (1500 V for a gap of about 15 mm).

Efficiency of ethanol to synthesis gas conversion reaches up to 95%. Hydrogen production is about 1.2 liters per minute; syngas production is 2 liters per minute. Energy efficiency, defined as the ratio of the energy released at syngas combustion to the electricity energy consumed for the discharges maintenance, is about 1.85. The energy costs per molecule of hydrogen are approximately 3 eV.

Numerical modeling of conversion kinetics at discharge conditions was performed using the Konnov model. Calculated data are in a good agreement with experimental data for gas mixture composition and hydrogen conversion degree. It proves that ethanol to synthesis gas conversion process in non-self sustained atmospheric-pressure DC discharge has a thermal nature.

References

- [1] Migun A.N., Chernukho A.P., Zhdanok S.A., *J. Eng. Phys. Thermophys.* 79, 651 (2006)
- [2] Conte E., Boulouchos K., *SAE Tech. Pap.* 2004-01-0972 (2004)
- [3] Bromberg L., Cohn D.R., Rabinovich A., Heywood J., *Int. J. Hydrogen Energ.* 26, 1115 (2001)
- [4] Isherwood K., Linna J., Loftus P., *SAE Tech. Pap.* 980939 (1998)
- [5] Green J. et al., *SAE Tech. Pap.* 2000-01-2206 (2000)
- [6] Petitpasa G., Rolliera J.-D., Darmonb A., Gonzalez-Aguilara J., Metkemeijera R., Fulcheria L., *Int. J. Hydrogen Energ.* 32, 2848 (2007)
- [7] Yukhymenko V.V., Verovchuk M.O., Olshevskii S., Chernyak V.Ya., Zrazhevskij V.A., Demchina V.P., et al., *Probl. At. Sci. Tech.: Plasma Phys.* 15, 128 (2009)
- [8] Zhdanok S.A., Krauklis A.V., Samtsov P.P., Suvorov A.V., *J. Eng. Phys. Thermophys.* 79, 1051 (2006)
- [9] Tatarova E., Bundaleska N., Dias F.M., Tsyganov D., Saavedra R., Ferreira C.M., *Plasma Sources Sci. T.* 22, 065001 (2013)
- [10] Akishev Yu., Grushin M., Kochetov I., Karal'nik V., Napartovich A., Trushkin N., *Plasma Sources Sci. T.* 14, S18 (2005)
- [11] Jasinski M., Dors M., Mizeraczyk J., *Eur. Phys. J. D* 54 179 (2009)
- [12] Arkhipenko V.I., Kirillov A.A., Callegari T., Safronau Y.A., Simonchik L.V., *IEEE T. Plasma Sci.* 37, 740 (2009)
- [13] Arkhipenko V.I., Callegari Th., Safronau Ya.A., Simonchik L.V., *IEEE T. Plasma Sci.* 37, 1297 (2009)
- [14] Chernukho A.P., Migun A.N., Zhdanok S.A., Rostaing J.C., Perrin J., *J. Eng. Phys. Thermophys.* 78, 394 (2005)
- [15] Konnov A., 28-th Symposium (Int.) on Combustion, Edinburgh, Abstr. Symp. Pap. p. 317 (2000)
- [16] Arkhipenko V.I., Kirillov A.A., Safronau A., Simonchik L.V., *Eur. Phys. J. D* 60, 455 (2010)
- [17] Arkhipenko V.I., Zgirouski S.M., Karoza A.G., Kirillov A.A., Simonchik L.V., *J. Appl. Spectrosc.* 80, 99 (2013)
- [18] Bretzlaaff R.S., Bahder T.B., *Revue Phys. Appl.* 21, 833 (1986)
- [19] Seymour E.F.W., Cotts R.M., Williams W.D., *Phys. Rev. Lett.* 35, 165 (1975)
- [20] Rothman L.S. et al., *JQSRT*, 2013, 130, 4